Nucleation, Growth, and Stabilization of Bose-Einstein Condensate Vortex Lattices

A. A. Penckwitt and R. J. Ballagh
Department of Physics, University of Otago, Dunedin, New Zealand

C. W. Gardiner
School of Chemical and Physical Sciences, Victoria University, Wellington, New Zealand
(Received 2 May 2002; published 11 December 2002)

We give a simple unified theory of vortex nucleation and vortex lattice formation in which (i) the thermal cloud plays a crucial role; (ii) the basic process is due to growth of the condensate from a rotating thermal cloud, which provides gain for certain surface modes of nonzero angular momentum; (iii) vortices appear initially as the result of a linear interference between the far fields of the condensate and the surface modes; and (iv) the description applies from the initiation process up to the final stabilization of the lattice. We have simulated the growth of vortex lattices from a rotating thermal cloud, and their production using a rotating trap.

DOI: 10.1103/PhysRevLett.89.260402 PACS numbers: 03.75.Fi

Recent experimental observations of vortex lattices in Bose-Einstein condensates [1–7] have focused attention on the *mechanisms* of vortex formation. For cases where the condensate is stirred by an anisotropic potential, the Gross-Pitaevskii equation has been used as the basis of a number of theoretical analyses. A perturbative calculation [8–10] of the mixing of the ground and excited condensate states by the stirring potential gives a critical rotation speed at which the mixing becomes effective. It is then argued that an instability will lead to growth of the vortex state. However, a nonperturbative calculation for a localized rotating stirrer [11] shows that in this case the mixing is predominantly between the ground state and an $l = 1$ vortex state, and that, as the relative amplitudes evolve by coherent "Rabi cycling," the full condensate exhibits a vortex cycling from infinity to the central regions of the condensate. No coherent mixing mechanisms, however, can explain the formation of a *vortex lattice,* since an energy barrier exists between the superposition state and the vortex lattice state, and some dissipative mechanism is required to remove the energy liberated when the vortex lattice is formed.

Haljan *et al.* [3] produced vortices by evaporatively cooling a rotating vapor of cold atoms. In this experiment, which involves no stirring potential, the mechanism of formation of the vortices must involve a modification of the theory of condensate growth [12] to take account of the nonzero angular momentum of the vapor from which the condensate is formed. We will show that the mechanism thus demonstrated is the fundamental process in those experiments in which the stirring of the condensate apparently generates a vortex lattice. Weak stirring, in the absence of any thermal cloud, produces only Rabi cycling of angular momentum in and out of the condensate. However, if the stirring also produces a rotating thermal cloud, then, by the same process responsible for the growth of a condensate [13], angular momentum is transferred *irreversibly* into the condensate, leading in equilibrium to a rotating vortex lattice. In general terms, this has already been noted in [14], and Williams *et al.* [15] showed how interactions with a thermal vapor cloud would give rise to an instability of surface modes, as required to produce vortices.

We have previously [16] derived a very simplified vortex growth equation with a broadly similar basis to that of Williams *et al.* This gives rise to an equation [given as Eq. (3)] which can describe the full process of vortex nucleation, growth, and stabilization. Using this equation, we show below how the growth of vortex lattices can be understood as a condensate growth process, and that the criterion for vortex nucleation is simply the condition that the gain in the growth process be positive. We also demonstrate explicitly how the vortices produced in the Rabi cycling caused by a rotating trap nucleate the growth process, which then proceeds to dominate the vortex lattice formation process.

The Gross-Pitaevskii equation for $\psi_R = \exp(i\mathbf{\Omega} \cdot \mathbf{L}t/\hbar)\psi$, the condensate wave function in a frame of reference rotating with angular velocity $\mathbf{\Omega}$, takes the form

$$i\hbar \frac{\partial \psi_R}{\partial t} = \left(-\frac{\hbar^2}{2m}\nabla^2 + V_T^R + u|\psi_R|^2 - \mathbf{\Omega} \cdot \mathbf{L} \right)\psi_R, \quad (1)$$

where $V_T^R(\mathbf{x})$ is the trap potential in the rotating frame. A vortex lattice results from the stationary solutions of Eq. (1) satisfying $i\hbar\partial\psi_R/\partial t = \mu_C\psi_R$ [17–19], which are normally obtained by integrating the Gross-Pitaevskii equation along an imaginary time direction [19]. [Indeed, Tsubota *et al.* [20] proposed an *ad hoc* modification of this method as a phenomenological model of the process of vortex lattice formation.]

Origin of dissipation.—When the condensate is grown from a rotating vapor cloud the growth process itself is dissipative, and in the experiments of [1–4] dissipation can arise by transfer of atoms between the thermal cloud and the condensate. The vortex growth equation derived

in [16] uses quantum kinetic theory for the growth of the wave function for a condensate trapped in a potential $V_T(\mathbf{x}, t)$ rotating with angular velocity $\mathbf{\Omega}$, from a thermal cloud held at temperature T and chemical potential μ and rotating with angular velocity $\boldsymbol{\alpha}$. A dissipative term arises from collisions between atoms in the thermal cloud trapped by the same potential as the condensate, in which one of the colliding atoms enters the condensate after the collision. The net rate of atom transfer as the result of such collisions is characterized by a coefficient

$$W^+(\mathbf{x}) = \frac{u^2}{(2\pi)^5\hbar^2}\int d^3\mathbf{K}_1 d^3\mathbf{K}_2 d^3\mathbf{K}_3\,\delta(\omega_{123}) \times \delta(\mathbf{K}_1 + \mathbf{K}_2 - \mathbf{K}_3)F_1F_2(1 + F_3) \quad (2a)$$

$$\approx g \times 4m(akT)^2/\pi\hbar^3, \quad (2b)$$

and in practice $g \approx 3$ fits most growth experiments. Here $F(\mathbf{x}, \mathbf{K})$ is the Bose-Einstein distribution function for a thermal cloud in an effective potential in the frame rotating at the *cloud's* angular velocity $\boldsymbol{\alpha}$. The vortex growth equation takes the form in the frame rotating with the *trap potential*

$$i\hbar\frac{\partial\psi_R}{\partial t} = \left(-\frac{\hbar^2}{2m}\nabla^2 + V_T^R(\mathbf{x}) + u|\psi_R|^2 - \mathbf{\Omega}\cdot\mathbf{L}\right)\psi_R + i\gamma\left(\mu + (\boldsymbol{\alpha} - \mathbf{\Omega})\cdot\mathbf{L} - i\hbar\frac{\partial}{\partial t}\right)\psi_R, \quad (3)$$

where $\gamma \equiv \hbar W^+/kT$. It is important to distinguish between the *cloud's* angular velocity $\boldsymbol{\alpha}$ and the *trap's* angular velocity $\mathbf{\Omega}$. If these are different the distribution of the thermal cloud is not truly thermodynamic equilibrium. In fact it is difficult to spin up a thermal cloud using a rotating potential; one therefore expects that $\alpha < \Omega$. In this Letter, however, we consider mainly the cases in which either the trap is cylindrically symmetric, so that we may set $\mathbf{\Omega} = 0$, or in which the cloud and the trap rotate at the same velocity, so $\boldsymbol{\alpha} = \mathbf{\Omega}$. Equation (3) is essentially equivalent in terms of the physical assumptions required for its derivation to that of [15], although its appearance is very different. In contrast, although Eq. (3) looks similar to that of [20], it is in fact very different, as explained in [16].

Simulation results for rotating vapor.—If we start with no initial condensate (apart from some seeding to start the growth process) a *nonrotating* condensate grows very rapidly. The vortex nucleation process then commences, and Fig. 1 shows a representative time sequence of two-dimensional simulations of Eq. (3) for a rotationally symmetric harmonic trap of frequency ω. The initial condensate is in the ground state of the trap, has unit norm, and chemical potential $\mu_C = 12.7\hbar\omega$. We simulate the nonstimulated collisions which start the process by adding to the intial wave function a uniform superposition of angular momentum states with $l = 1$ to 30 on a Gaussian radial profile centered at the Thomas-Fermi radius and with maximum amplitude $\sim 2 \times 10^{-7}$.

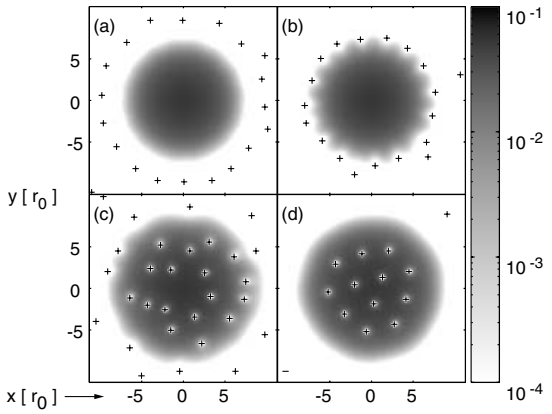

FIG. 1. Condensate density during formation of vortex lattice from a rotating thermal cloud. Vortices are marked by + or −: (a) $t = 29.28t_0$; (b) $t = 37.70t_0$; (c) $t = 52.40t_0$; (d) $t = 187.24t_0$. Condensate wave function seeded as described in text. Parameters are $\alpha = 0.65\omega$, $\mu = 12\hbar\omega$, $\gamma = 0.1$, $u = 1000u_0$, and initial $\mu_C = 12.7\hbar\omega$. Units are time $t_0 = 1/\omega$, distance $r_0 = \sqrt{\hbar/2m\omega}$, and collisional strength $u_0 = \hbar\omega r_0^2$.

Figure 1(a) is a density plot of the condensate near the end of the first stage of the evolution, in which an imperfect ring of 19 vortices arrives from infinity to just outside the Thomas-Fermi radius. As this ring shrinks further [Fig. 1(b)], several vortices are shed, and a dominant ring of 16 vortices passes through the Thomas-Fermi radius into the interior of the condensate. These vortices then distribute themselves irregularly but quasiuniformly over the condensate which expands and picks up angular velocity [Fig. 1(c)]. Subsequently, over a long period, further vortices leave (and for larger values of α may enter) the dense region, until finally a regular lattice of 12 vortices rotating at angular velocity α in the laboratory frame remains [Fig. 1(d)].

The overall time scale of the process is illustrated in Fig. 2(a) which shows the total angular momentum increasing sharply around $t \approx 40$, when the 16 vortices enter the dense part of the condensate. For a given seeding, the time scale for this onset is determined by γ and to good approximation scales as γ^{-1}. The *local chemical potential* $\mu_{\rm loc}(\mathbf{x})$ [defined as the absolute value of the right-hand side of Eq. (1) divided by ψ_R] provides a useful characterization of the temporal development. In Fig. 2(b), we plot the evolution of the spatial mean of $\mu_{\rm loc}(\mathbf{x})$, which exhibits a rapid initial adjustment (to $\approx \mu$), as the condensate roughly equilibrates with the thermal cloud, and a later dip at $t \approx 48$ during which the number of atoms in the condensate increases [see Fig. 2(a)]. The spatial variance σ_μ of $\mu_{\rm loc}(\mathbf{x})$ quantifies the deviation of the solution from equilibrium (where it is zero). It becomes large as the vortices enter the dense region of the condensate, and its subsequent slow decay

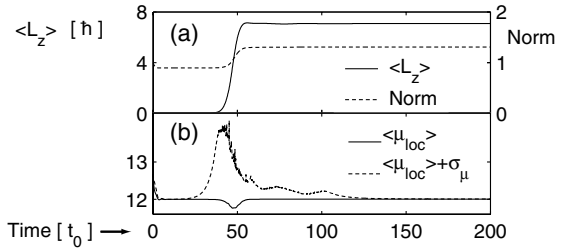

FIG. 2. Time evolution of condensate quantities for the case of Fig. 1. (a) $\langle L_z \rangle$ and norm; (b) $\langle \mu_{\rm loc} \rangle$ and σ_μ (in units of $\hbar\omega$).

indicates the long time needed for stabilization of the vortex lattice, which is approximately proportional to γ^{-1}, and hence to the temperature. We have found that the number of vortices in the stable final lattice increases with α and μ and is generally different from the number seen in the initial ring. It also exhibits a very weak dependence on the exact form of the seeding. For the case of $\mu = 12\hbar\omega$ the critical value for the appearance of any vortices is found from the simulations to be $\alpha = 0.444\,\omega$, at which speed an irregular ring of ten vortices appears initially, settling down eventually to three vortices in a lattice inside the Thomas-Fermi radius. Three-dimensional simulations of Eq. (3) also confirm the general behavior seen in Fig. 1.

Analytic treatment.—To understand the nucleation and growth process of the vortices we consider the linearized Bogolyubov excitations above the initial state with angular momentum l and energy eigenvalues $\epsilon_{n,l}$ measured relative to μ_C. From the final term of Eq. (3) we see that excitations for which $\epsilon_{n,l} < \mu - \mu_C + \hbar\alpha l$ will experience a positive growth rate $G \approx \gamma(\mu - \mu_C + \hbar\alpha l - \epsilon_{n,l})/\hbar$. Initially this causes rapid growth of the condensate (the $n = l = 0$ component, which has the lowest eigenvalue) until the condensate and thermal cloud approximately equilibrate ($\mu \approx \mu_C$). Subsequently, the gain of the other components is $\gamma(\alpha l - \epsilon_{n,l}/\hbar)$, and thus the critical value of α for positive gain is given by $\epsilon_{0,l} = \hbar\alpha l$, the same condition for criticality found in [15]. Above criticality, the dominant value l_v is that which maximizes the gain and is given by $\partial(\hbar\alpha l - \epsilon_{0,l})/\partial l = 0$. A crude estimate for l_v can be obtained by minimizing $\hbar^2 l^2/2mr^2 - \hbar\alpha l$ at the Thomas-Fermi (TF) surface, to give $l_v \approx \pi R_{\rm TF}^2 2m\alpha/h$. This equals the number of vortices which would result from filling a disk of radius $R_{\rm TF}$ with a vortex lattice [21]. In the initial stages of vortex formation, when the process is still linear, the wave function of the condensate takes the form (for simplicity including only the excitation with maximum gain, which has angular momentum $\hbar l_v$ and energy $\hbar\omega_v \equiv \hbar\alpha l_v - \epsilon_{0,l_v}$)

$$\psi_R \approx e^{-i\mu_C t/\hbar}\{\xi_0 + e^{il_v\phi + Gt}[ue^{i\omega_v t} + ve^{-i\omega_v t}]\}. \quad (4)$$

Here $\xi_0(r)$ is the initial rotationally symmetric condensate wave function, ϕ is the azimuthal angle, and $u(r)$, $v(r)$ are obtained by solving the Bogolyubov–de Gennes equations. The essential behavior can be seen by neglecting $v(r)$, so that ψ has l_v zeros—that is, vortices—given by the interference of the two terms. These vortices all occur at the same radius, initially at infinity. Since the long distance behavior of $u(r)$ must be less rapid than that of $\xi_0(r)$, the ring will steadily shrink as the excitation grows. The time dependence of the coefficient means that the ring of vortices rotates at the angular frequency ω_v in the rotating frame. In a more detailed picture, more values of l should be included, and the corresponding superposition will be an imperfectly circular ring of vortices.

The analytic treatment can be verified by decomposing the condensate into angular momentum components and plotting the occupation values P_l against time, as in Fig. 3(a). We see that the l components above threshold grow exponentially up to the time $t \approx 40$ (when the vortex ring passes through the Thomas-Fermi radius), and the gain is maximum for $l_v = 16$. In Fig. 3(b) we compare the gain prediction $\gamma(\alpha l - \epsilon_{0,l}/\hbar)$ (obtained by calculating the surface modes $\epsilon_{0,l}$ for a condensate with $\mu_C = 12\hbar\omega$) against the gain rates measured from the simulation. Our gain prediction is very accurate, and we also find that the spatial particle density for each l component matches the prediction from the corresponding Bogolyubov wave function.

Rotating trap, no thermal cloud.—Finally, we consider the connection between stirring and growth. As an example of a case of pure stirring we have simulated a rotating elliptical trap in the absence of a thermal cloud. The general behavior is well represented by the case $\mu_C = 12.7\hbar\omega$ and $\Omega = 0.65\,\omega$, for which we find that the condensate deforms into an elliptical shape rotating at the trap frequency with a similarly deformed ring of about 28 vortices in the low density region. The resulting state is a distorted version of Fig. 1(a) [22], and this subsequently undergoes an oscillatory behavior, but with no further penetration of the vortices into the condensate. Only the even angular momentum components of

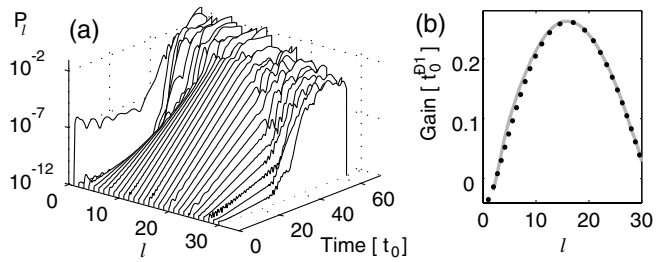

FIG. 3. (a) Evolution of angular momentum occupation probabilities P_l for $l = 1$ to 30 for the case of Fig. 1. (b) Comparison of gain coefficients of l components obtained from the simulation in Fig. 1 (solid line) with the predicted gain coefficients $G = \gamma(\alpha l - \epsilon_{0,l}/\hbar)$ (dotted line).

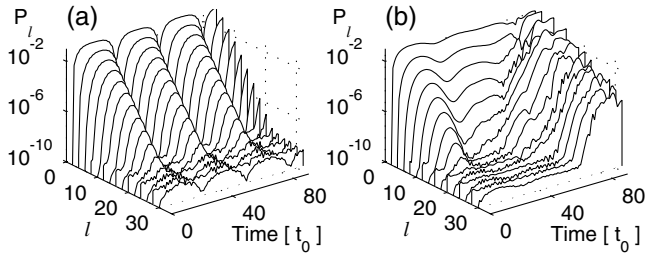

FIG. 4. Evolution of angular momentum occupation probabilities P_l for (a) rotating elliptical trap with no thermal cloud ($\gamma = 0$) and (b) rotating elliptical trap and corotating thermal cloud. Only the even l states are shown. Parameters as in Fig. 1 except trap parameters $\omega_x^2 = 1.05\omega^2$, $\omega_y^2 = 1.15\omega^2$, and $\alpha = \Omega = 0.65\omega$.

the condensate become significantly occupied and undergo periodic cycling [Fig. 4(a)]. This can be well understood in terms of the Rabi cycling model [11], noting that an elliptical potential can connect the initial ground state only to states of even l. Resonant mixing to the surface modes will occur when $\hbar\Omega l - \epsilon_{0,l} = 0$, and the lowest value of Ω for which this occurs [when also $\partial(\hbar\Omega l - \epsilon_{0,l})/\partial l = 0$] gives the same condition for criticality as found in Refs. [9,10]. This is also exactly the same condition as for the rotating cloud.

Rotating trap with thermal cloud.—Now repeating this simulation, but with a thermal cloud [Eq. (3) with $\alpha = \Omega$ and $\gamma \neq 0$], we get dramatically different results. The same elliptical distortion of the condensate occurs, but the effect tends to smooth out with time. A distorted vortex ring appears, with an initial number of vortices as expected from the growth mechanism (here ≈ 14), and then shrinks into the condensate and nucleates the vortex lattice, initially penetrating the condensate at its narrowest radius. The angular momentum projections in Fig. 4(b) show the difference very clearly. The vortex lattice is the result of the growth process, which is essentially superposed on the effects of stirring, eventually masking them. This leads us to suggest that the principal effect of the rotating trap in experiments [1,2,4–7] is to produce a rotating thermal cloud, which then transfers angular momentum into the condensate, eventually forming the vortex lattice. In contrast, using a nonrotating thermal cloud gives no vortices, as expected from the gain analysis given above.

Conclusions.—In our simple unified theory of the nucleation and formation of vortex lattices, the thermal cloud is a crucial feature, leading to an analysis of vortex formation in terms of the growth in occupation of modes with nonzero angular momentum. Vortices appear initially as the result of a linear interference between the far fields of the surface modes with nonzero angular momentum and the condensate and proceed from infinity towards the bulk of the condensate, where they rearrange themselves into a stable lattice. Simply stirring a condensate in the absence of a thermal cloud does not lead to a vortex lattice; however, in the presence of a thermal cloud, stirring can seed angular momentum components which may then grow from the thermal cloud by stimulated collisions. The critical angular velocity of the thermal cloud to allow growth is the same as the critical angular velocity required for stirring to resonantly mix surface modes with the condensate, and it agrees with the latter values calculated by previous workers [9,10,15]. However, our treatment goes beyond the instability point and includes the full dynamics of lattice stabilization.

This work was supported by the Marsden Fund of New Zealand under Contract No. PVT-902.

[1] K. W. Madison, F. Chevy, W. Wohlleben, and J. Dalibard, Phys. Rev. Lett. **84**, 806 (2000).
[2] K. W. Madison, F. Chevy, and J. Dalibard, Phys. Rev. Lett. **86**, 4443 (2001).
[3] P. C. Haljan, I. Coddington, P. Engels, and E. A. Cornell, Phys. Rev. Lett. **87**, 210403 (2001).
[4] C. Raman *et al.*, Phys. Rev. Lett. **87**, 210402 (2001).
[5] J. R. Abo-Shaeer, C. Raman, J. M. Vogels, and W. Ketterle, Science **292**, 476 (2001).
[6] J. R. Abo-Shaeer, C. Raman, and W. Ketterle, Phys. Rev. Lett. **88**, 070409 (2002).
[7] E. Hodby *et al.*, Phys. Rev. Lett. **88**, 010405 (2001).
[8] A. L. Fetter, Phys. Rev. A **64**, 063608 (2001).
[9] F. Dalfovo and S. Stringari, Phys. Rev. A **63**, 011601(R) (2001).
[10] J. R. Anglin, Phys. Rev. Lett. **87**, 240401 (2001).
[11] B. M. Caradoc-Davies, R. J. Ballagh, and K. Burnett, Phys. Rev. Lett. **83**, 895 (1999).
[12] M. J. Davis and C. W. Gardiner, J. Phys. B **35**, 733 (2002).
[13] C. W. Gardiner, P. Zoller, R. J. Ballagh, and M. J. Davis, Phys. Rev. Lett. **79**, 1793 (1997).
[14] O. N. Zhuravlev, A. E. Muryshev, and P. O. Fedichev, Phys. Rev. A **64**, 053601 (2001).
[15] J. E. Williams *et al.*, Phys. Rev. Lett. **88**, 070401 (2002).
[16] C. W. Gardiner, J. R. Anglin, and T. I. A. Fudge, J. Phys. B **35**, 1555 (2002).
[17] A. L. Fetter and A. A. Svidinsky, J. Phys. Condens. Matter **13**, R135 (2001).
[18] D. L. Feder, C. W. Clark, and B. I. Schneider, Phys. Rev. A **61**, 011601(R) (2000).
[19] D. L. Feder, C. W. Clark, and B. I. Schneider, Phys. Rev. Lett. **82**, 4956 (1999).
[20] M. Tsubota, K. Kasamatsu, and M. Ueda, Phys. Rev. A **65**, 023603 (2002).
[21] R. J. Donnelly, *Quantized Vortices in Helium II* (Cambridge University Press, Cambridge, 1991).
[22] Movies showing these results are available from http://www.physics.otago.ac.nz/bec/lattice.